# Binary systems as dynamical detectors of stochastic gravitational waves
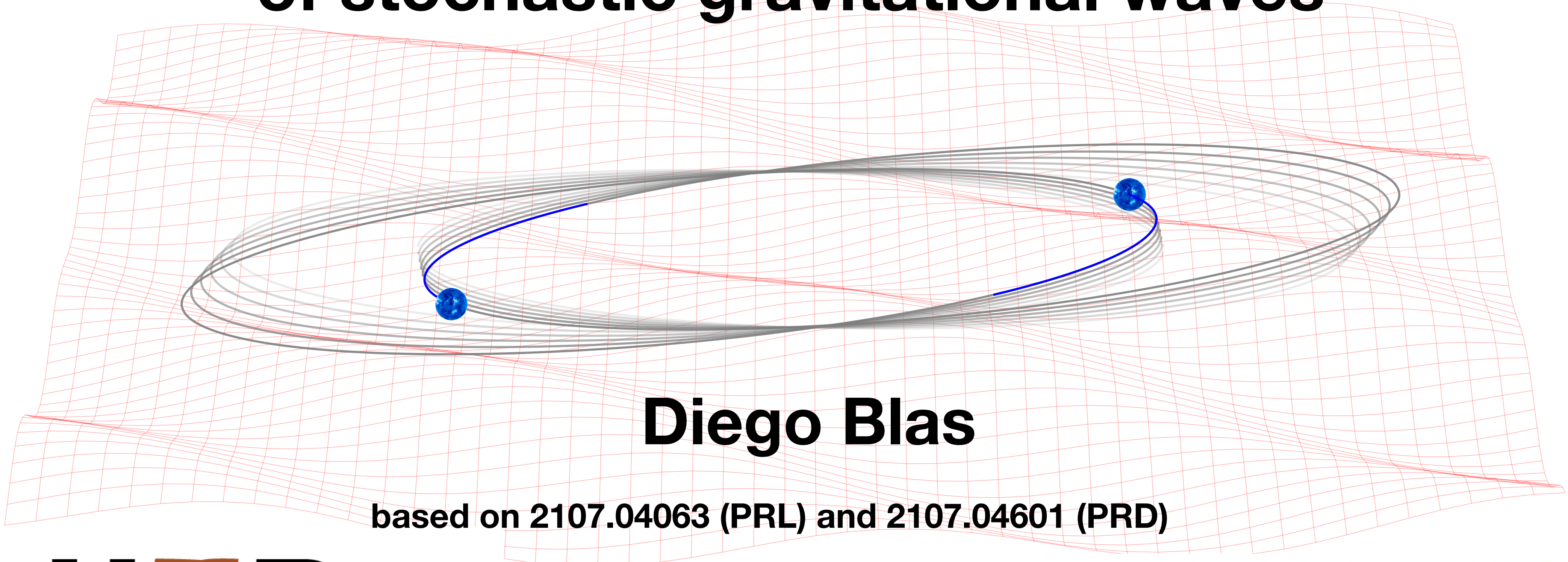


## Diego Blas

based on 2107.04063 (PRL) and 2107.04601 (PRD)

(w. Alex Jenkins, UCL)
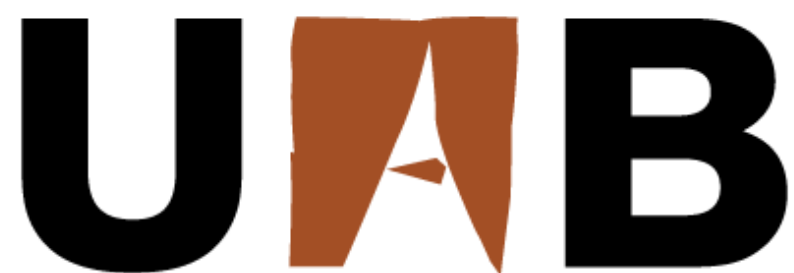
**UAB**
Universitat Autònoma
de Barcelona

**IFAE**
BIST Barcelona Institute of Science and Technology

# A taxonomy of GW signals
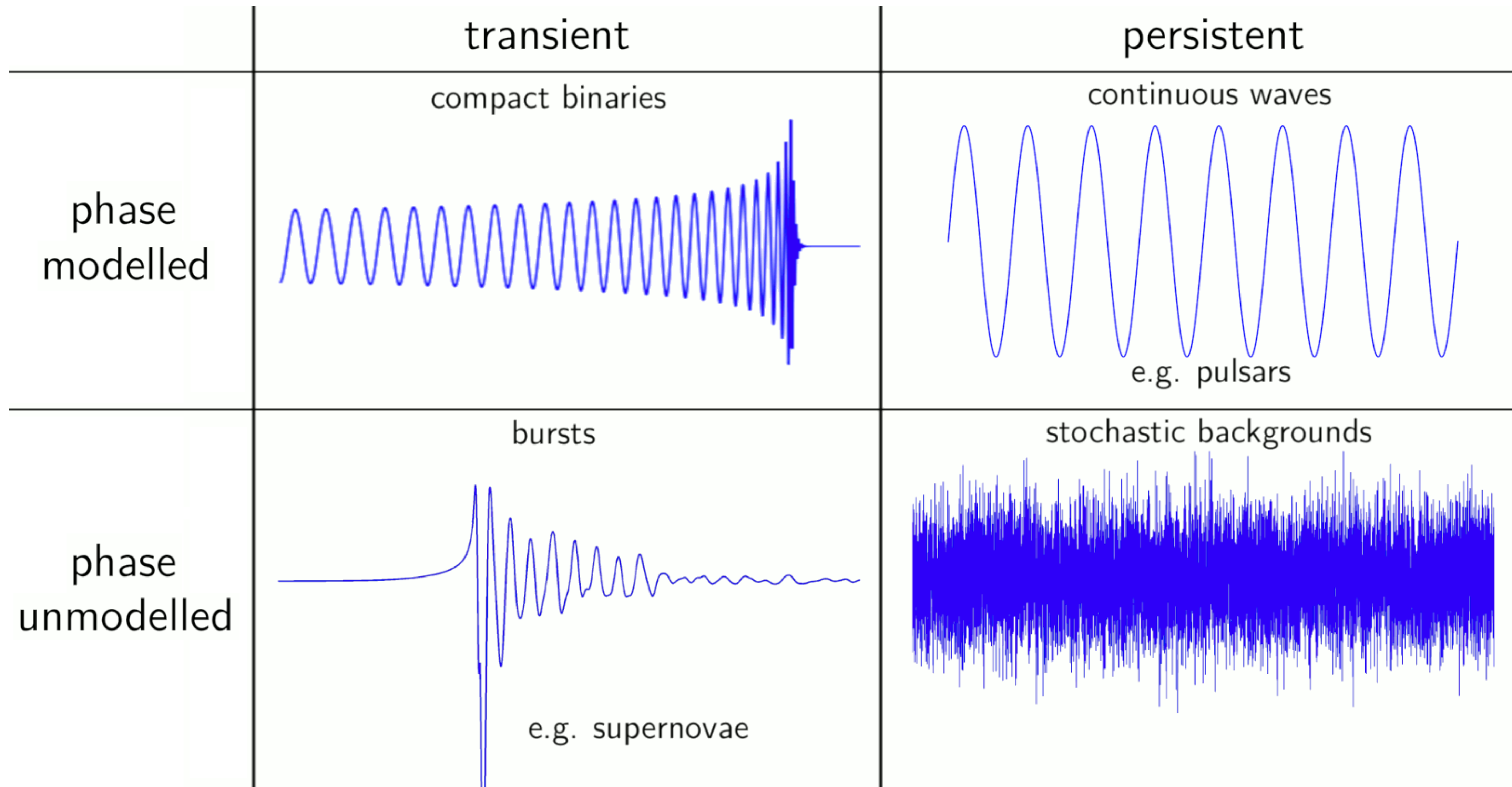
# Stochastic gravitational-wave background (SGWB)



Background

Foreground
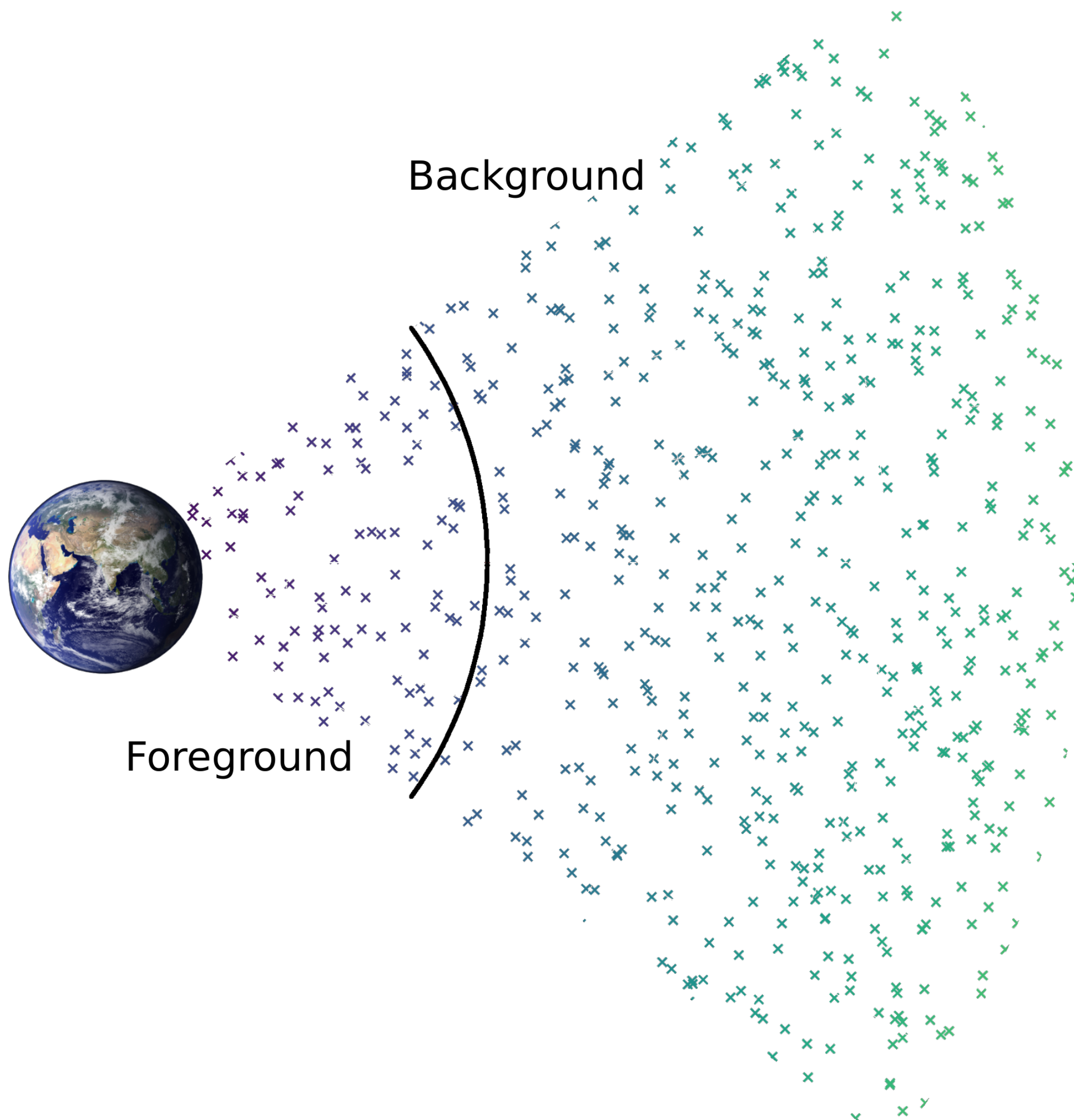
- incoherent, persistent GW signal
- faint/numerous sources
- astrophysical and cosmological
- GW density parameter:

$$\Omega_{\mathsf{GW}}(f) = \frac{1}{\rho_{\mathsf{crit}}} \frac{\mathrm{d}\rho_{\mathsf{GW}}}{\mathrm{d}(\ln f)}$$

# Current SGWB constraints

# Current SGWB constraints

# Current SGWB constraints

Detecting GWs with binary resonance
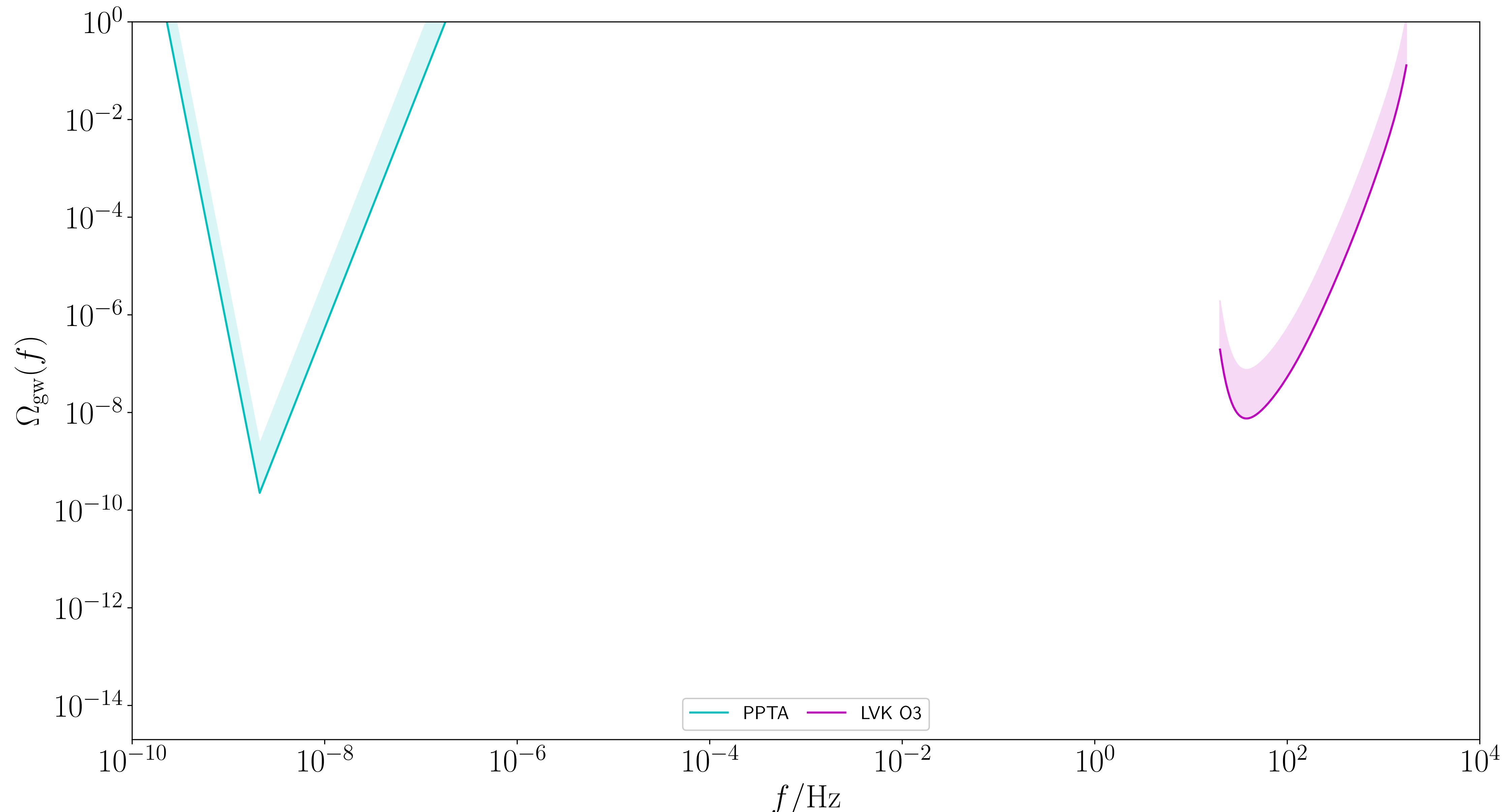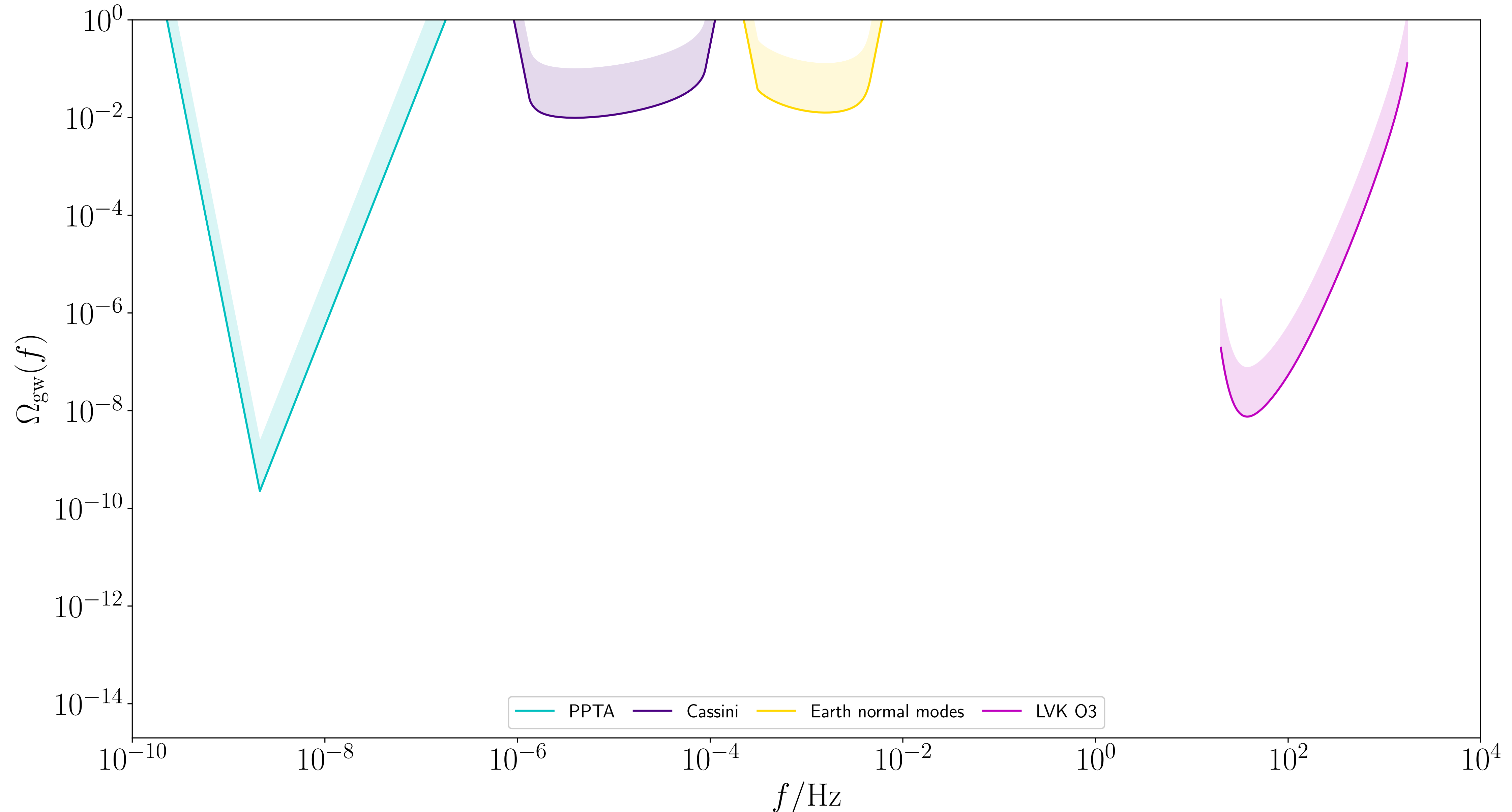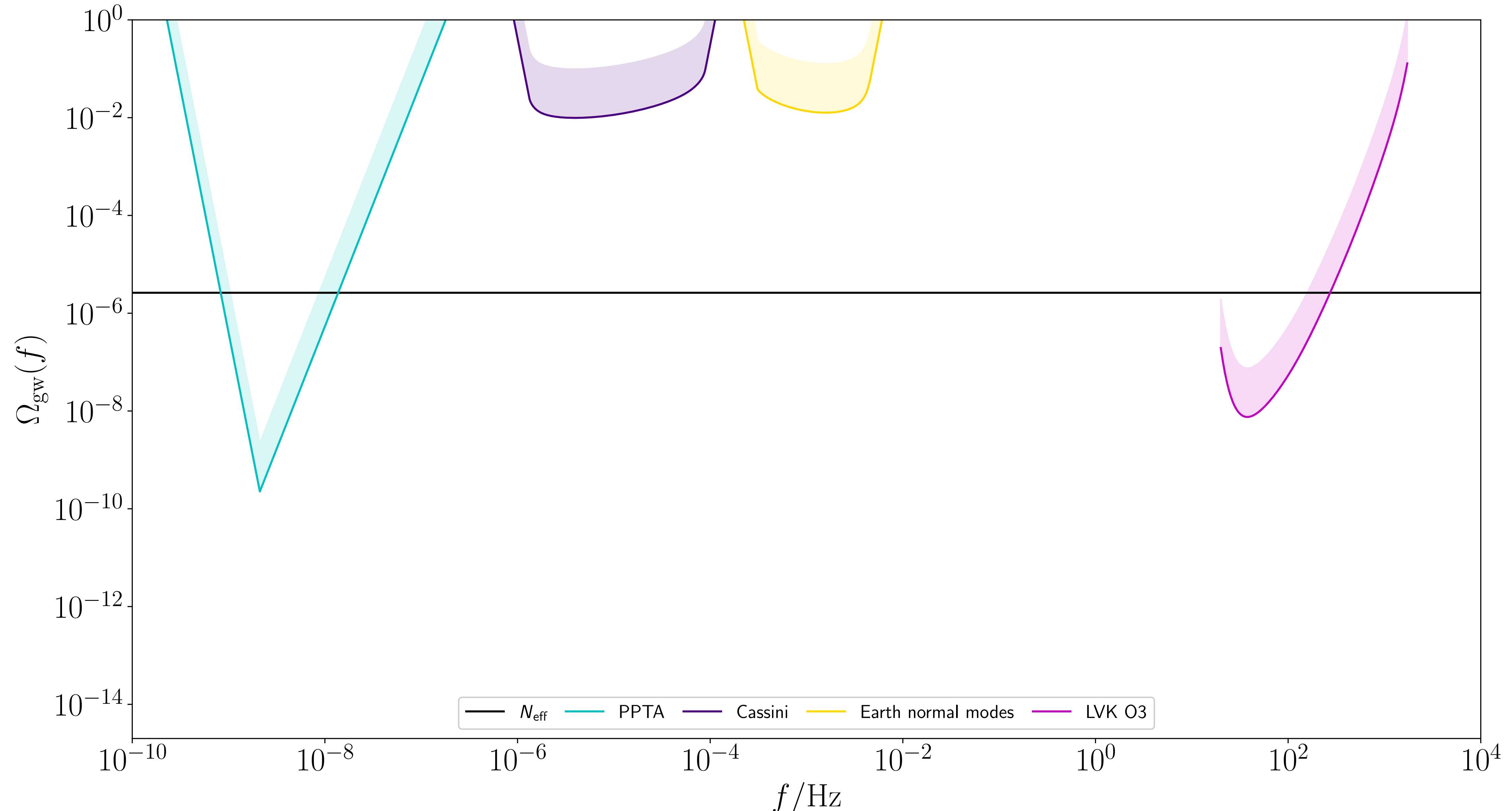
# Future SGWB constraints
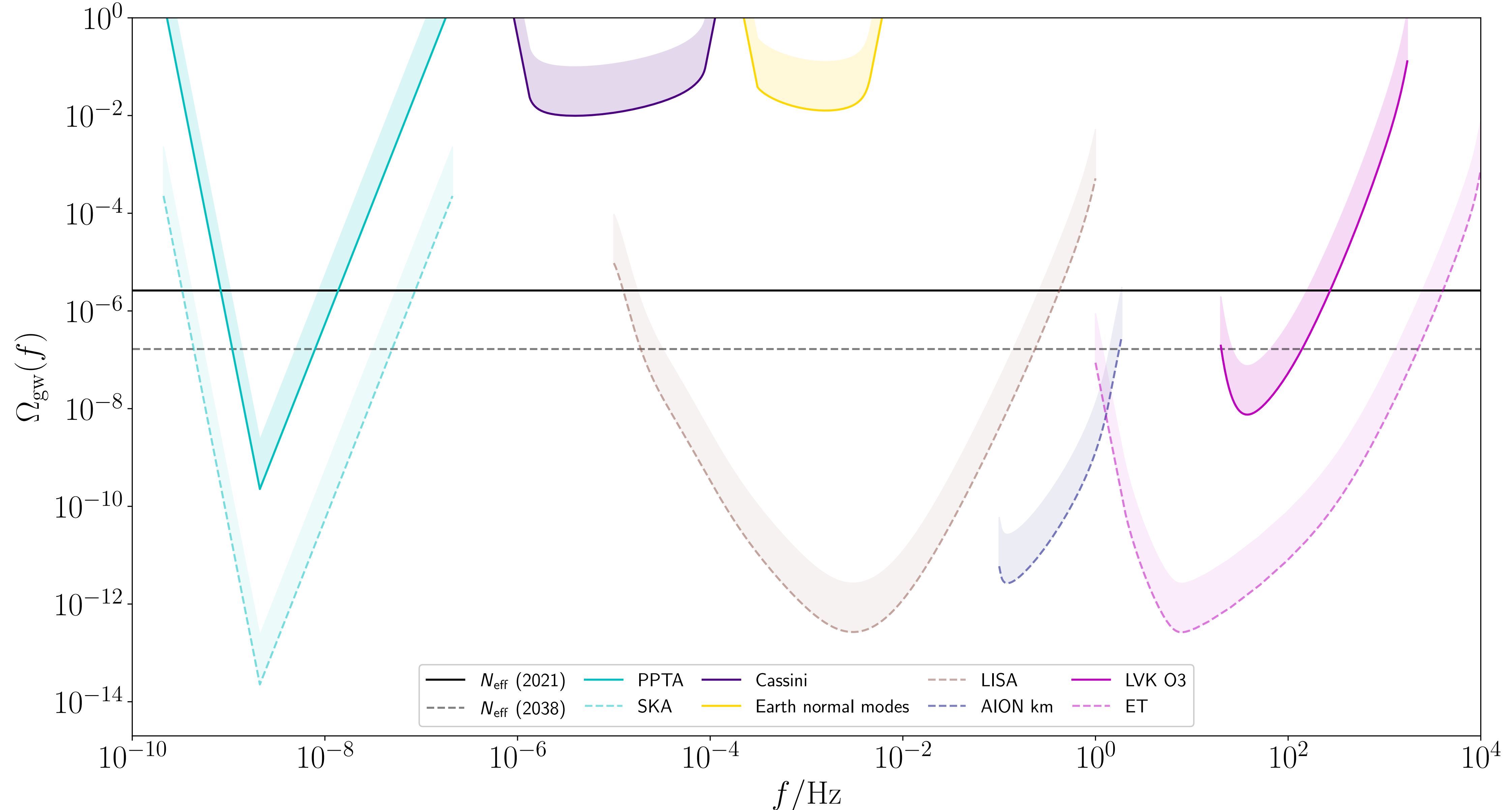
# Future SGWB constraints
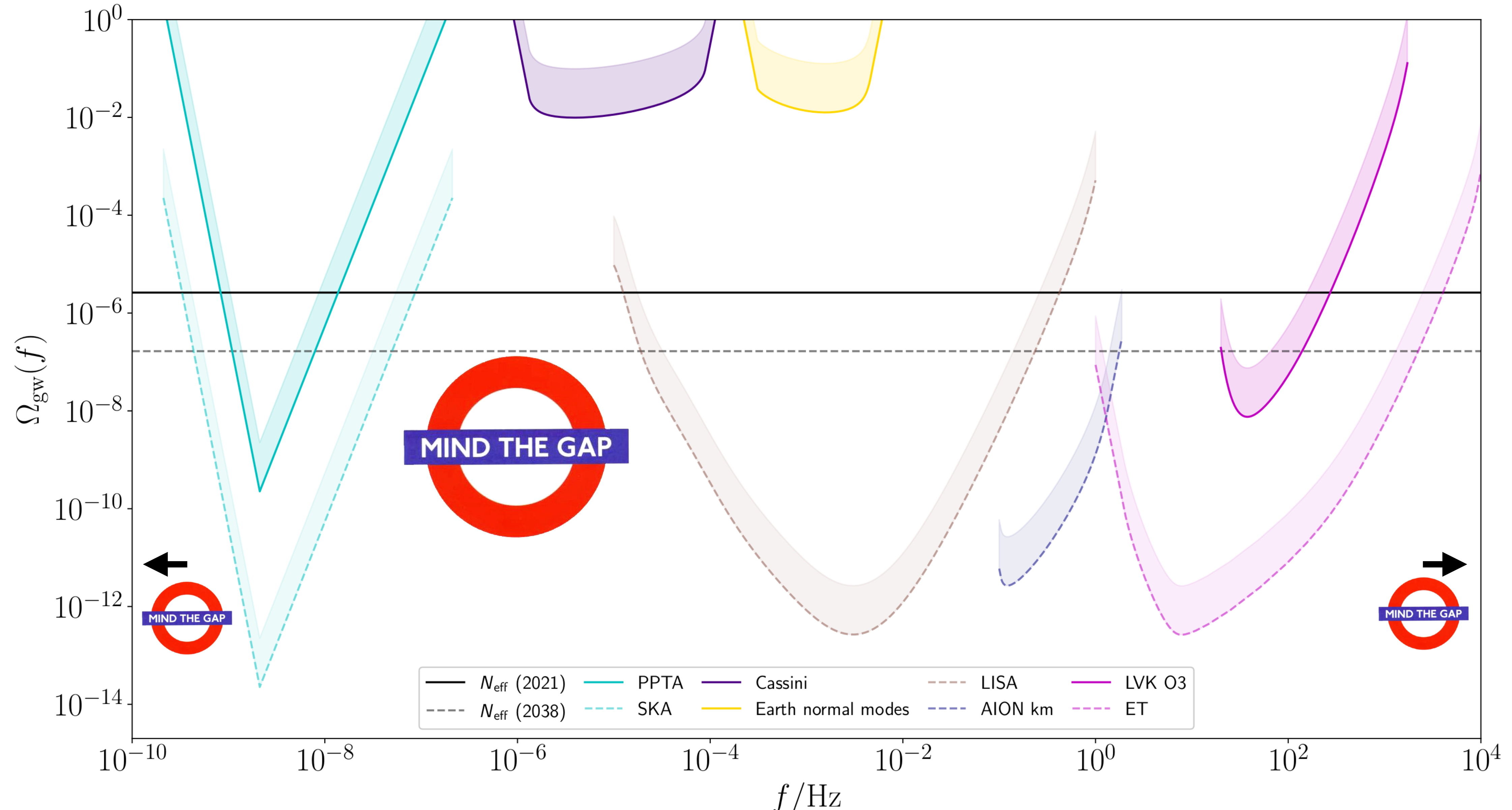
# A way forward: binary resonance
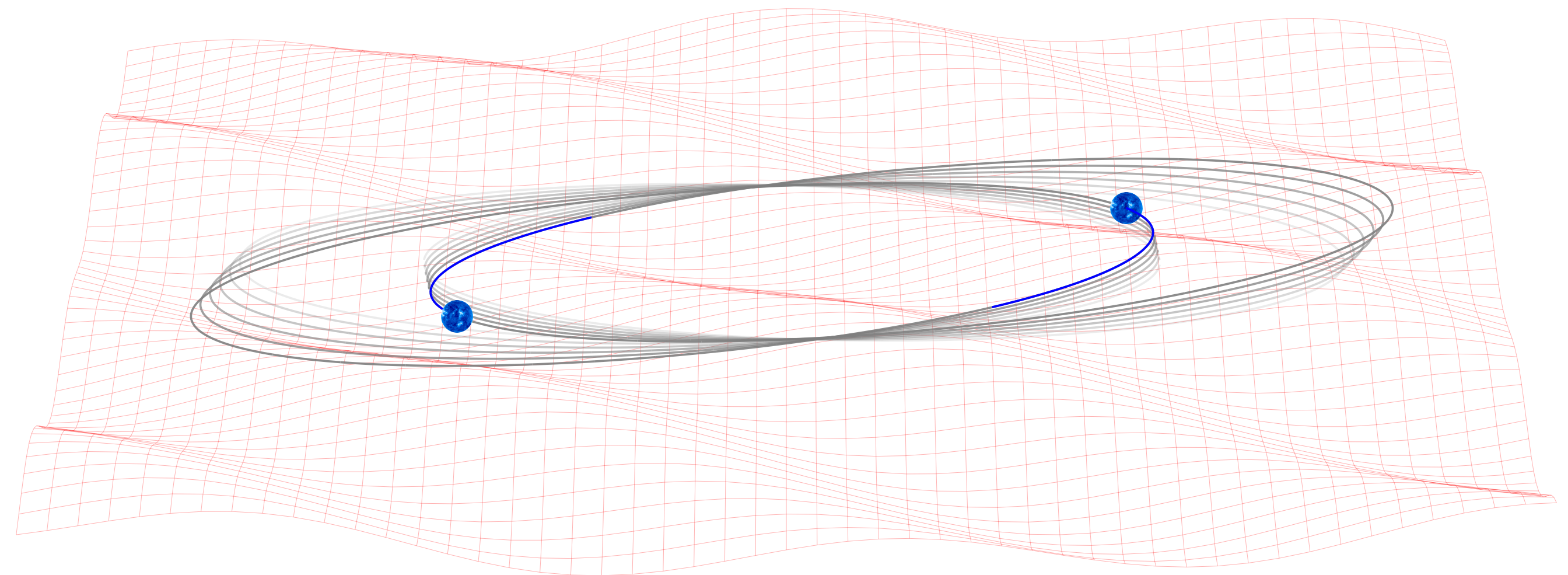


- GWs cause oscillations between orbiting bodies
- resonant for frequencies $f = n/P$, where $P$ is the period
- imprints on the orbit accumulate over time

# Orbital elements

- **period** $P$, **eccentricity** $e$:
  *size* and *shape* of orbit

- **inlination** $I$, **ascending node** $\Omega$:
  *orientation* in space

- **pericentre** $\omega$,
  **mean anomaly at epoch** $\varepsilon$:
  radial and angular *phases*
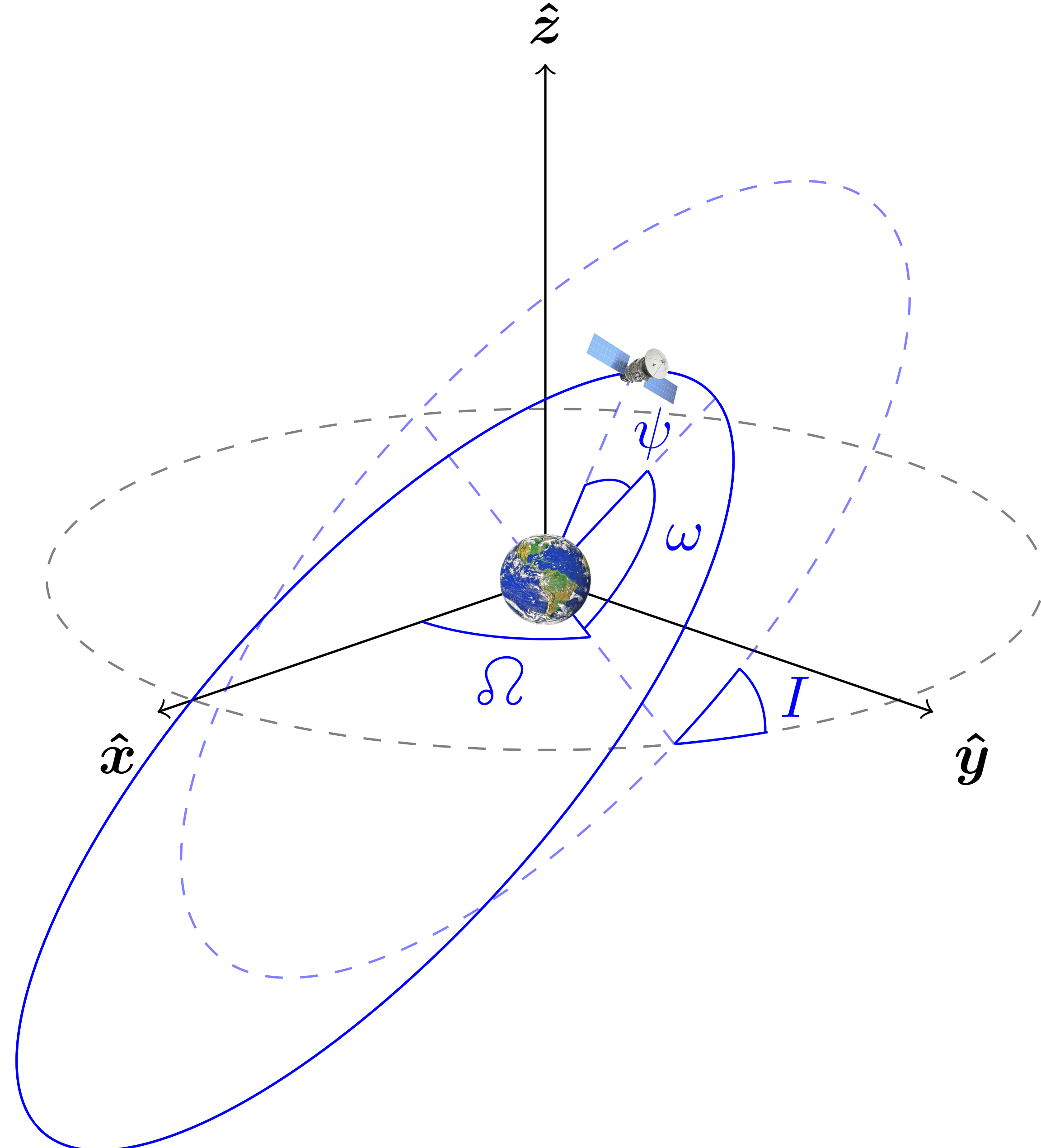
# Binary resonance: a brief history

discussed by Misner, Thorne, and Wheeler...

## 1. The Relative Motions of Two Freely Falling Bodies

As a gravitational wave passes two freely falling bodies, their proper separation oscillates (Figure 37.3). This produces corresponding oscillations in the redshift and round-trip travel times for electromagnetic signals propagating back and forth between the two bodies. Either effect, oscillating redshift or oscillating travel time, could be used in principle to detect the passage of the waves. Examples of such detectors are the Earth-Moon separation, as monitored by laser ranging [Fig. 37.2(a)]; Earth-spacecraft separations as monitored by radio ranging; and the separation between two test masses in an Earth-orbiting laboratory, as monitored by redshift measurements or by laser interferometry. Several features of such detectors are explored in exercises 37.6 and 37.7. As shown in exercise 37.7, such detectors have so low a sensitivity that they are of little experimental interest.

...but that was *50 years ago!*

investigated more recently by Lam Hui *et al*, PRD (2013),
similar ideas used to search for dark matter by Blas *et al*, PRL (2017)

## time for a closer look?

# Our new approach
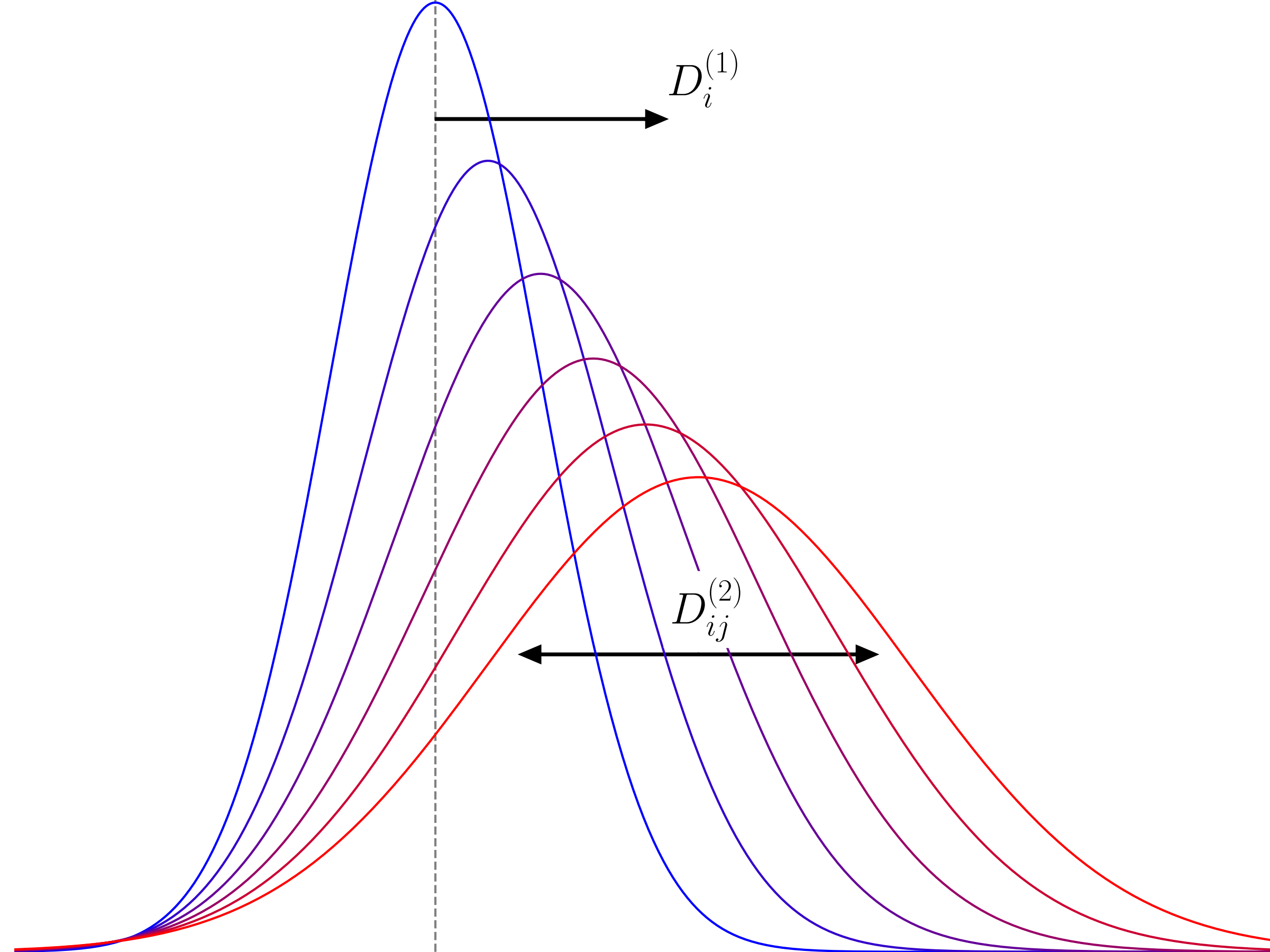


- track distribution function $W(\boldsymbol{X}, t)$ of orbital elements $\boldsymbol{X} = (P, e, I, \Omega, \omega, \varepsilon)$

- evolves through *Fokker-Planck eqn.*

$$\frac{\partial W}{\partial t} = -\frac{\partial}{\partial X_i}\big(D_i^{(1)} W\big) + \frac{\partial}{\partial X_i}\frac{\partial}{\partial X_j}\big(D_{ij}^{(2)} W\big)$$

- *drift* and *diffusion* coefficients

$$D_i^{(1)}(\boldsymbol{X}) = V_i(\boldsymbol{X}) + \sum_{n=1}^{\infty} \mathcal{A}_{n,i}(\boldsymbol{X})\,\Omega_{\mathrm{gw}}(n/P)$$

$$D_{ij}^{(2)}(\boldsymbol{X}) = \sum_{n=1}^{\infty} \mathcal{B}_{n,ij}(\boldsymbol{X})\,\Omega_{\mathrm{gw}}(n/P)$$

# Two binary probes

timing of binary pulsars

lunar and satellite laser ranging
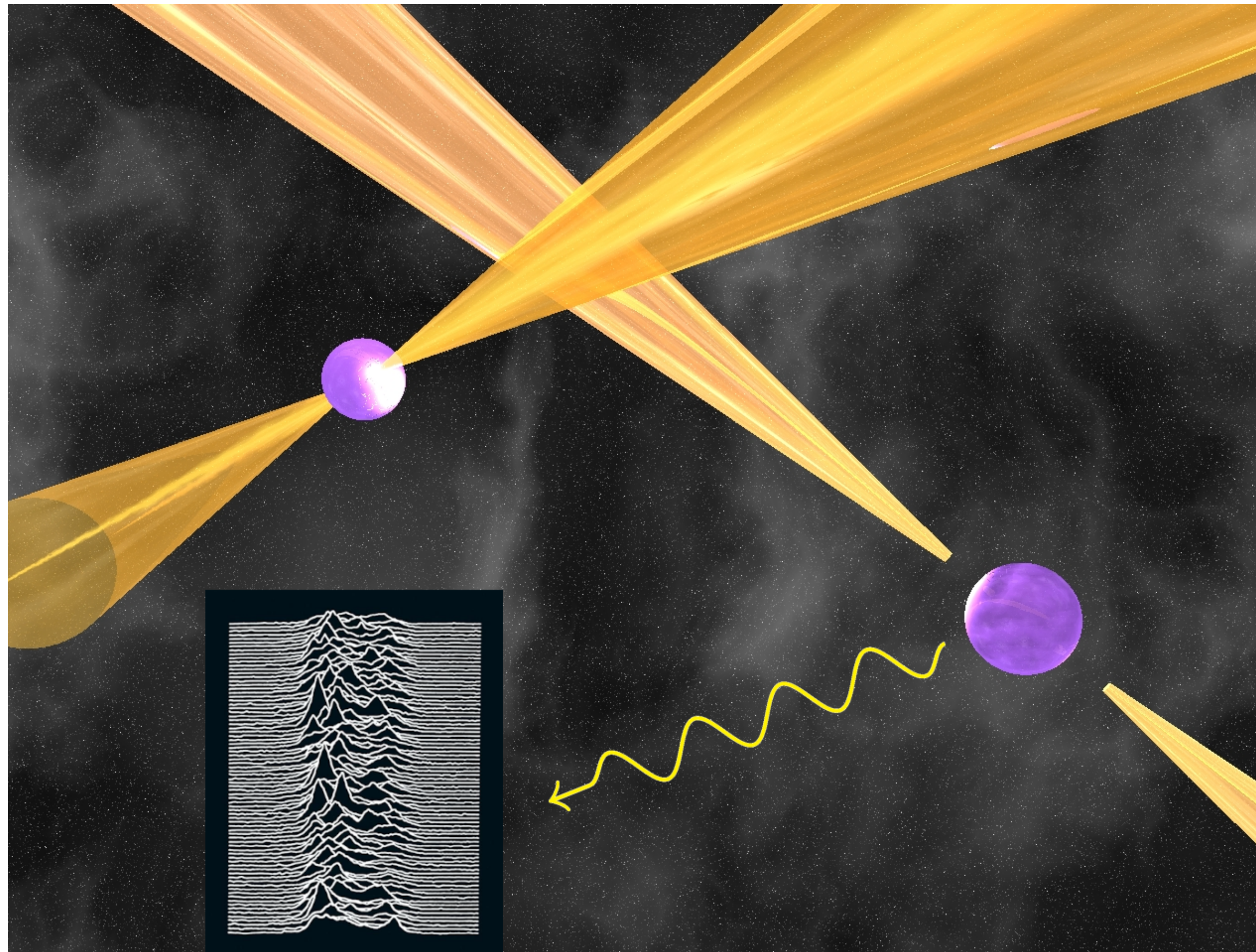


(pulsar animation credit: Michael Kramer)
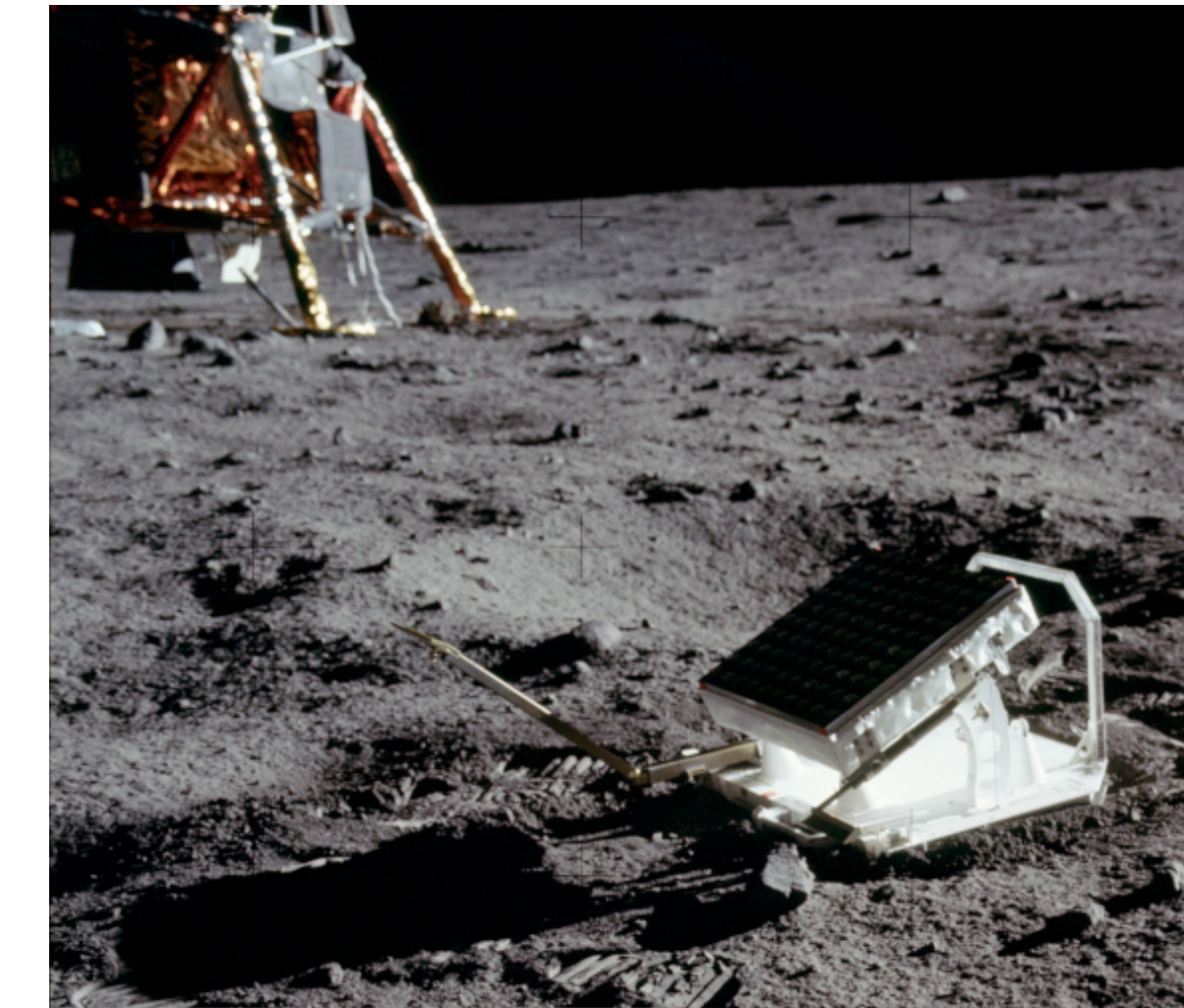
(image credit: NASA)

# Our forecast constraints

Detecting GWs with binary resonance
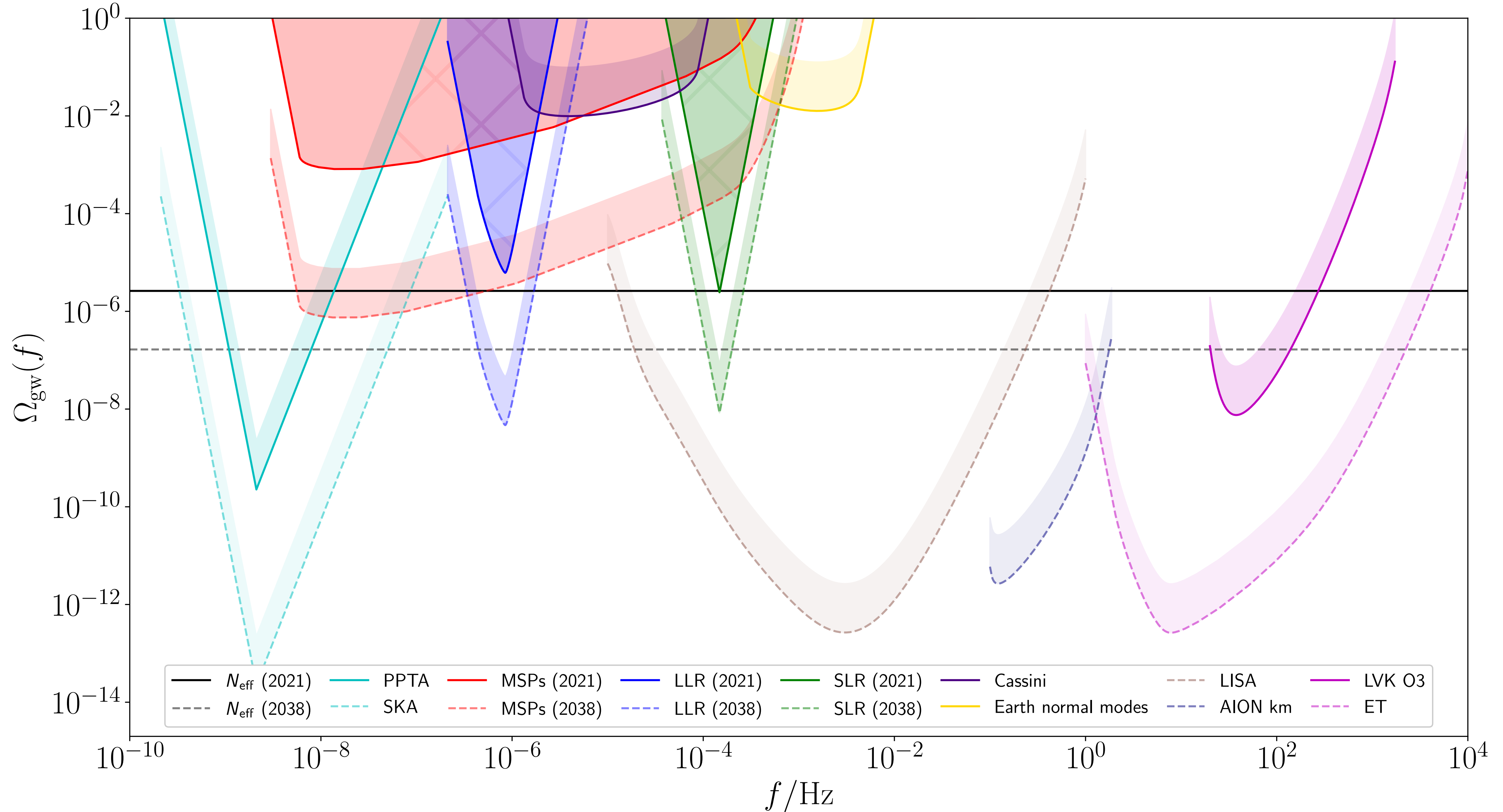
# Signals in the μHz band
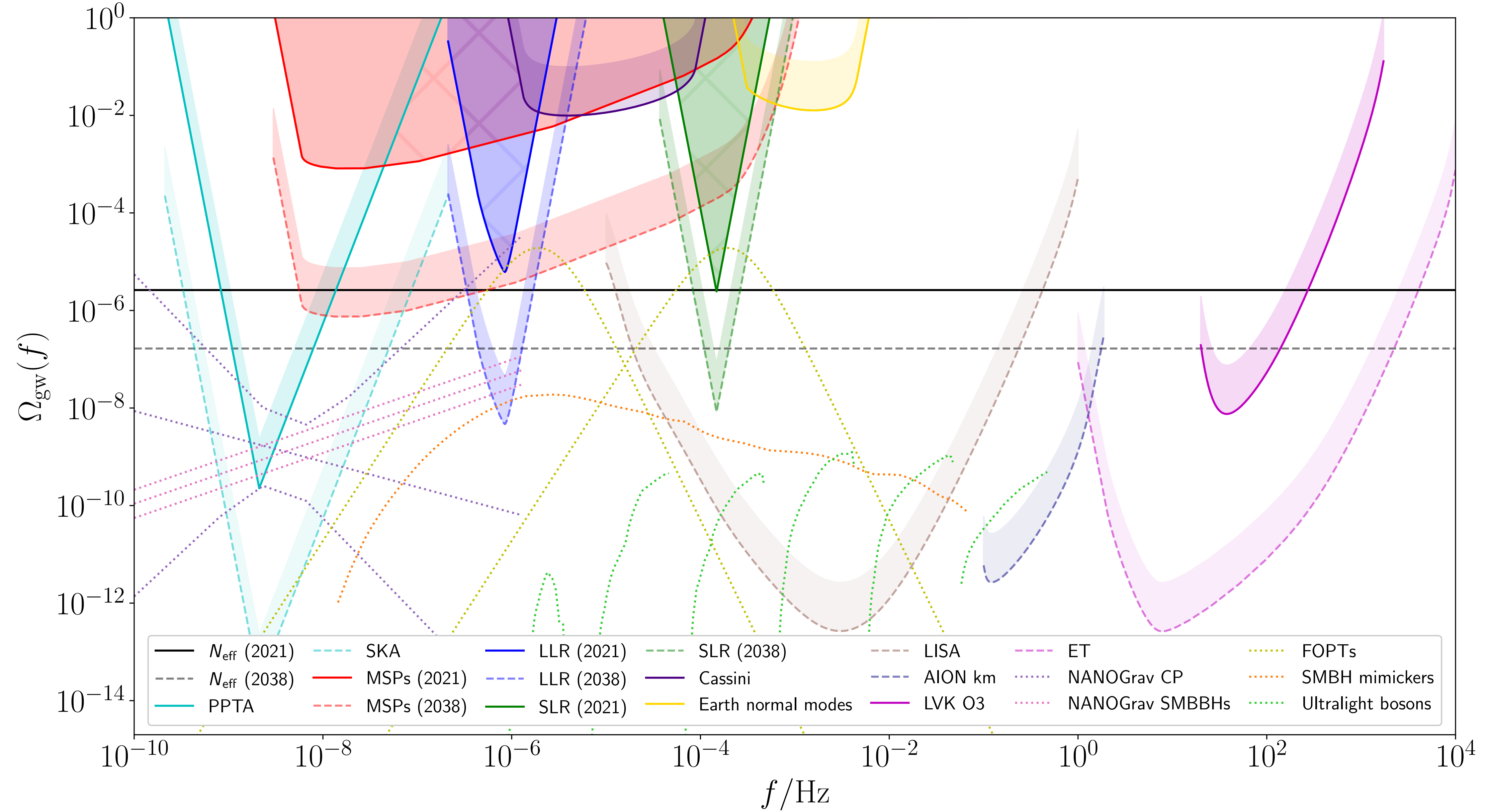
# An example signal: cosmological phase transitions



- key prediction of many particle physics models
- four parameters:
  - temperature $T_*$
  - strength $\alpha$
  - rate $\beta/H_*$
  - bubble-wall velocity $v_w$
- peak frequency

$$f_* \approx 19\,\mu\text{Hz} \times \frac{T_*}{100\,\text{GeV}} \frac{\beta/H_*}{v_w}$$

# Phase transition constraints



Legend:
- Lunar laser ranging (blue)
- Satellite laser ranging (green)
- Einstein Telescope (magenta)
- LISA (brown)
- Square Kilometre Array (cyan)
- $N_{\text{eff}}$ (CMB and BBN) (black)

Axes: $\log_{10}\alpha$, $\log_{10}\beta/H_*$, $v_w$, $\log_{10}(T_*/\text{GeV})$

Detecting GWs with binary resonance
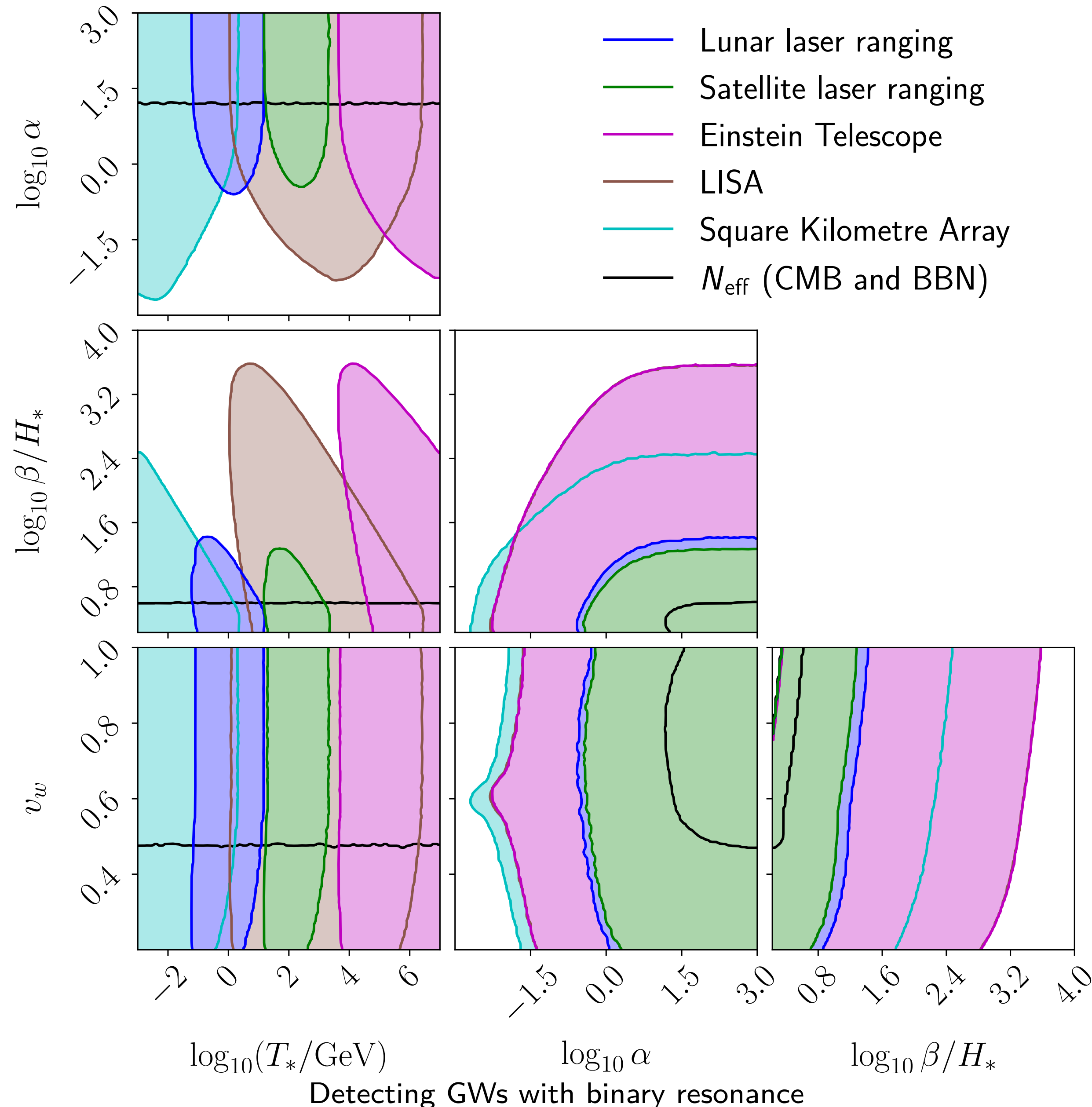
# Summary and outlook

- binary resonance can probe a unique GW frequency band
- we have developed a powerful new formalism
- unique constraints on phase transitions (and more)
- plenty more work to do! more signals, more systems, plus running on real data

*thanks for listening!*
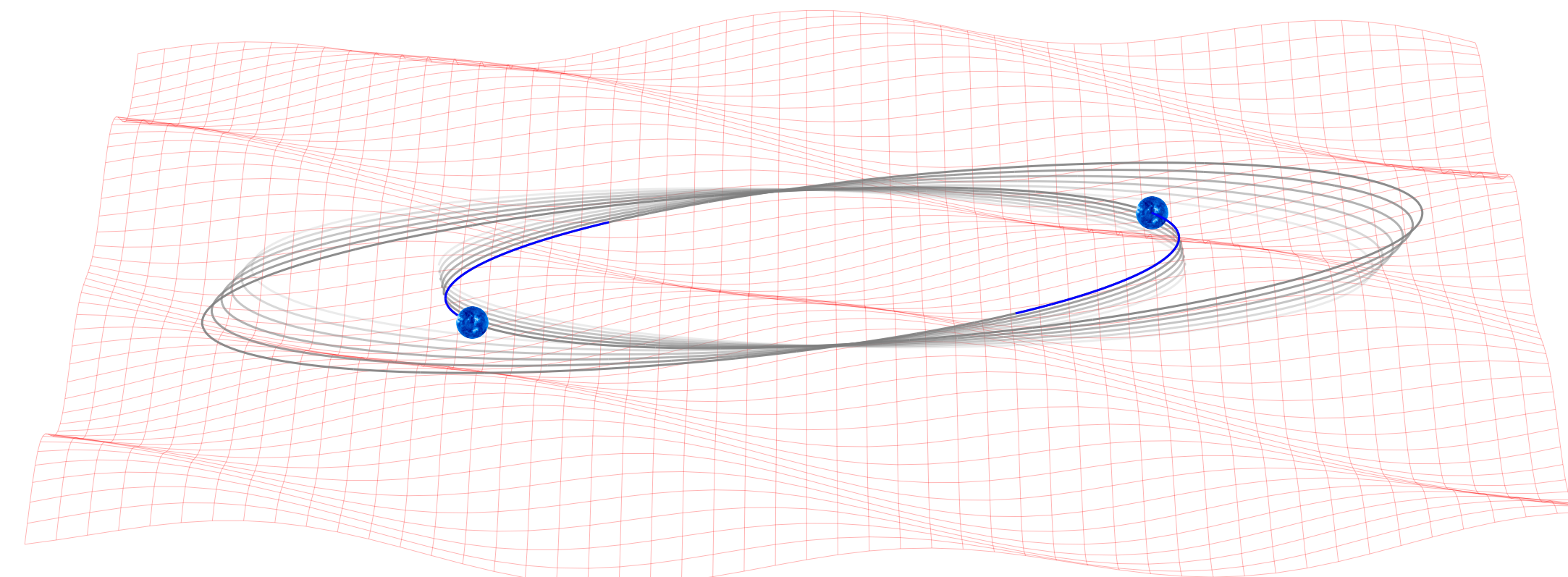
# The Gravitational Soundscape
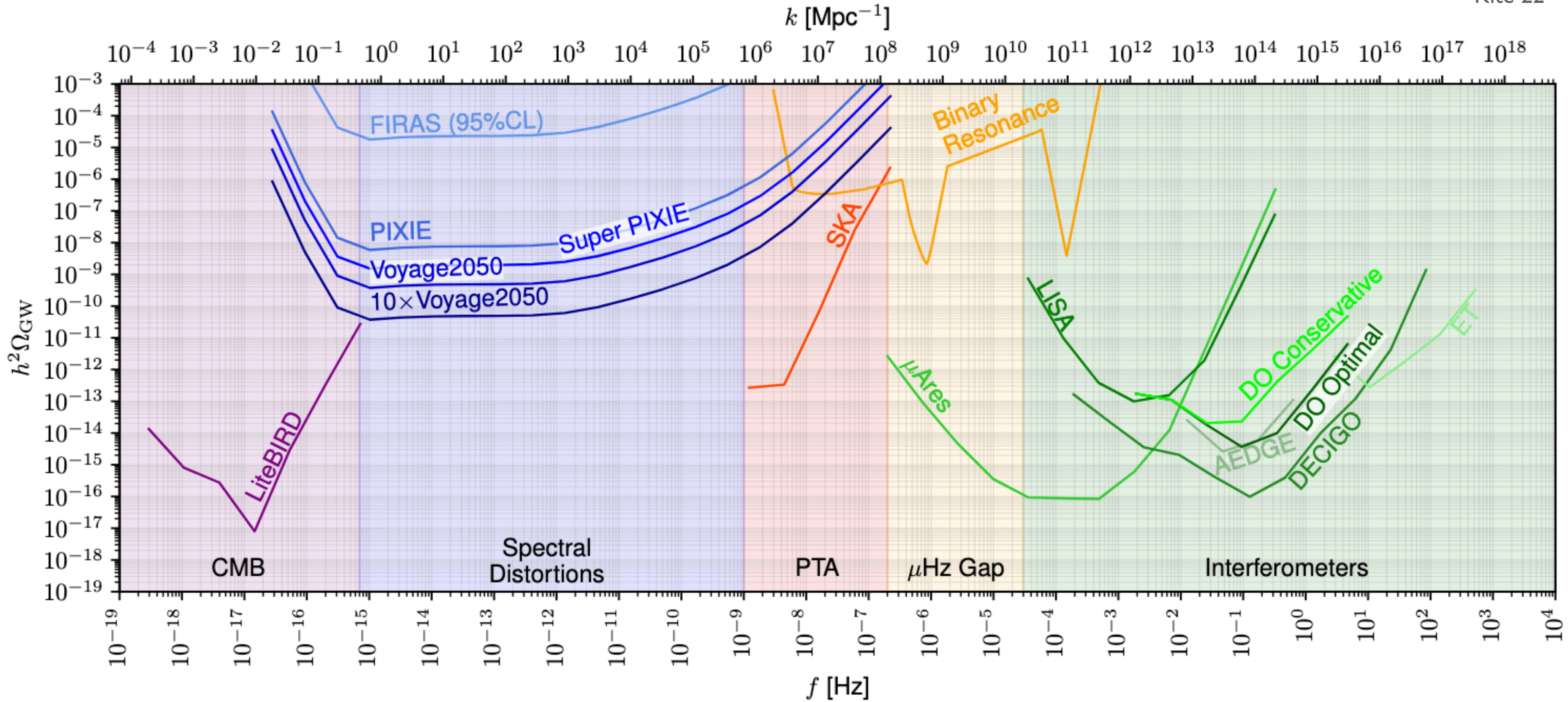
# Backup Slides
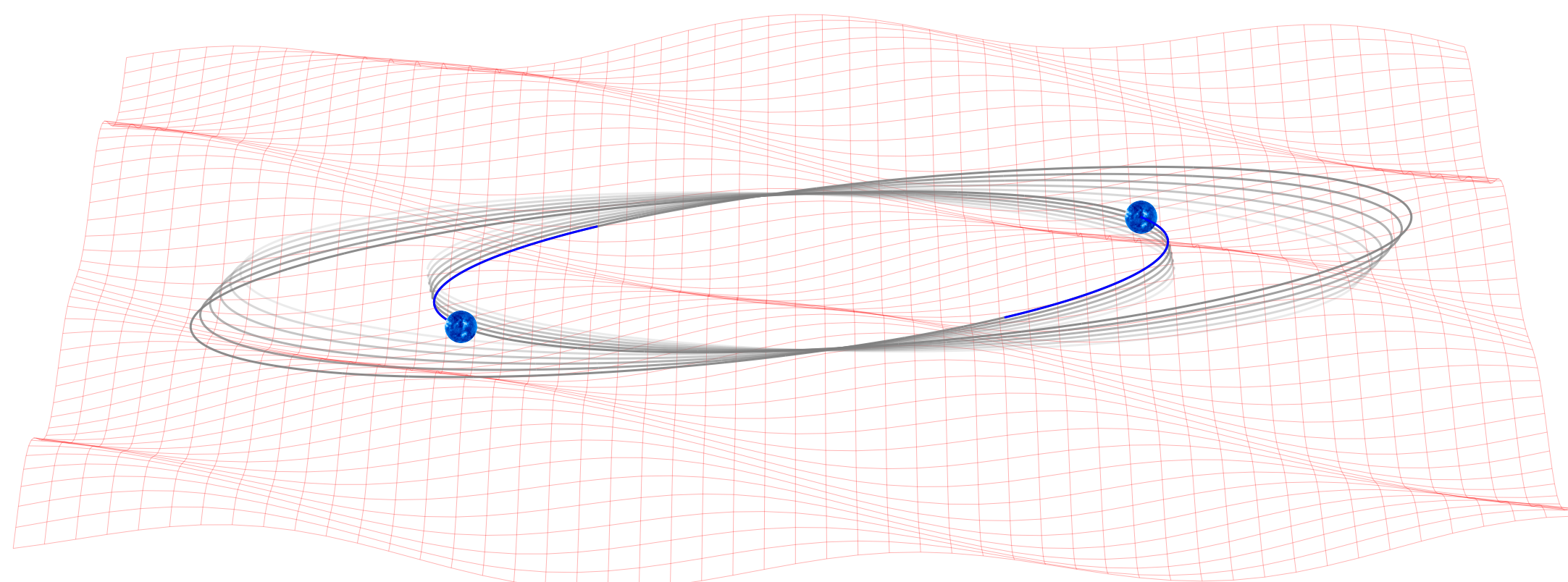
# Characteristic strain
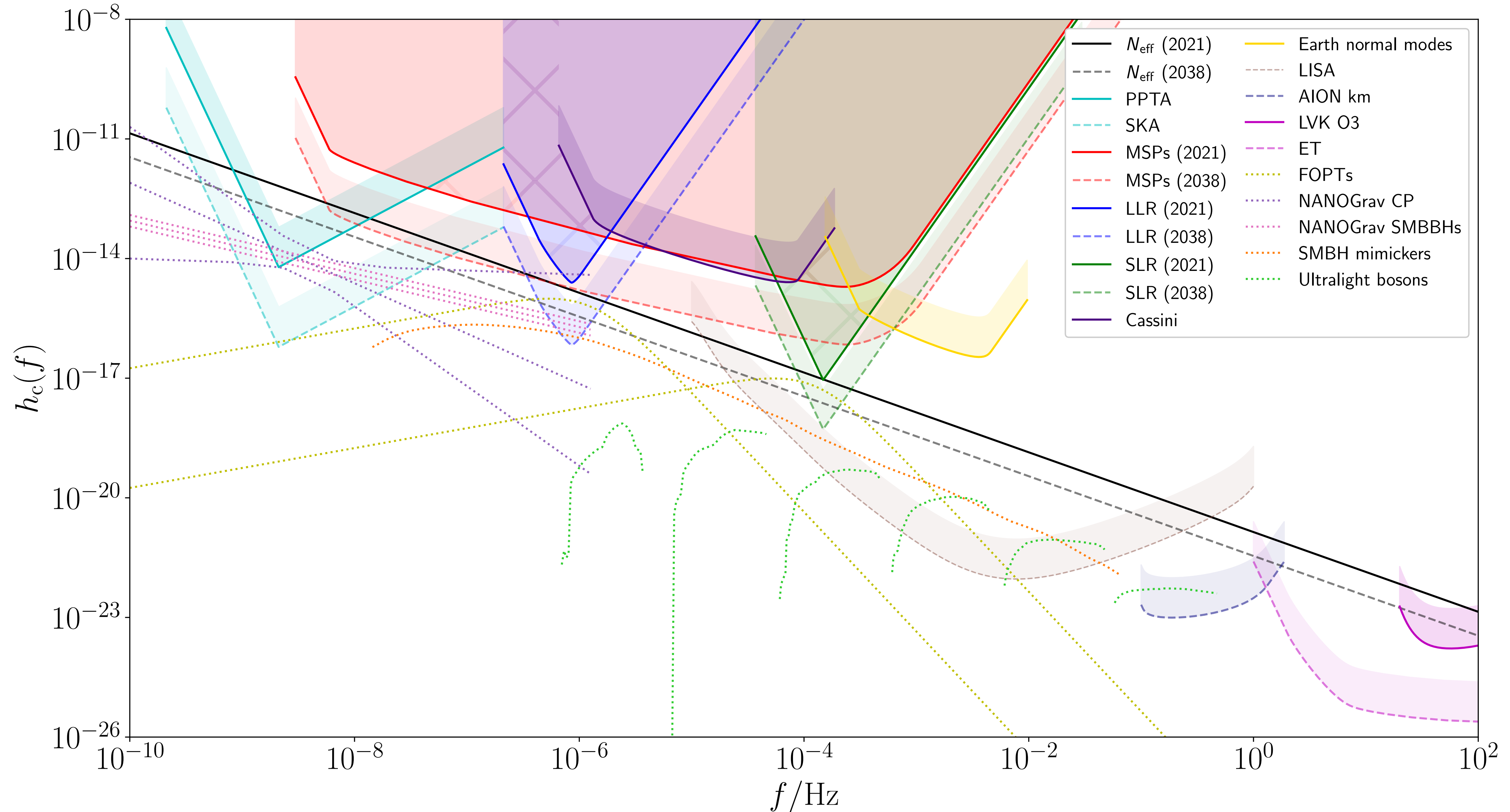
# Combining binary pulsar bounds
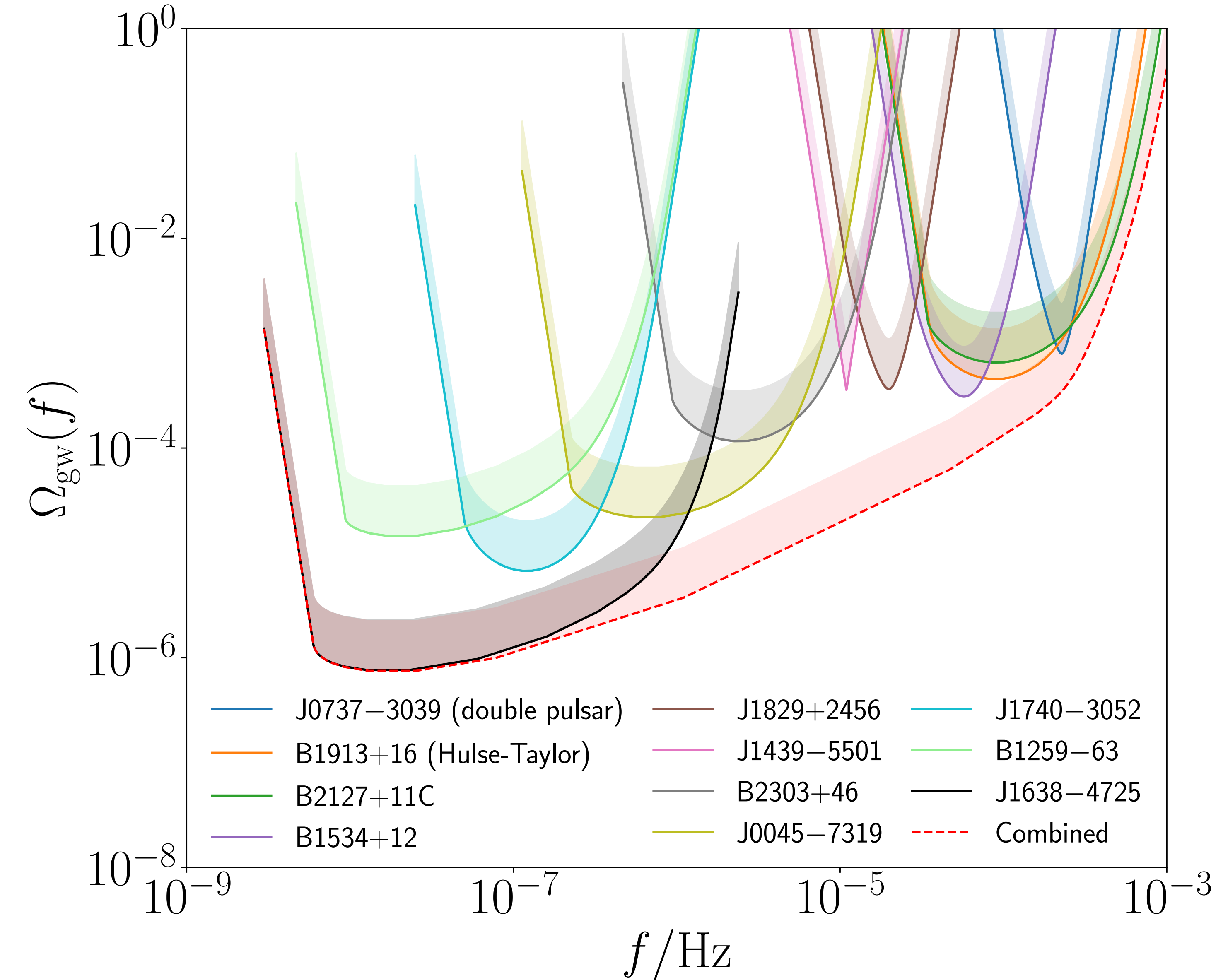
# Power-law sensitivity vs. monochromatic sensitivity

lunar laser ranging, $e \approx 0.055$
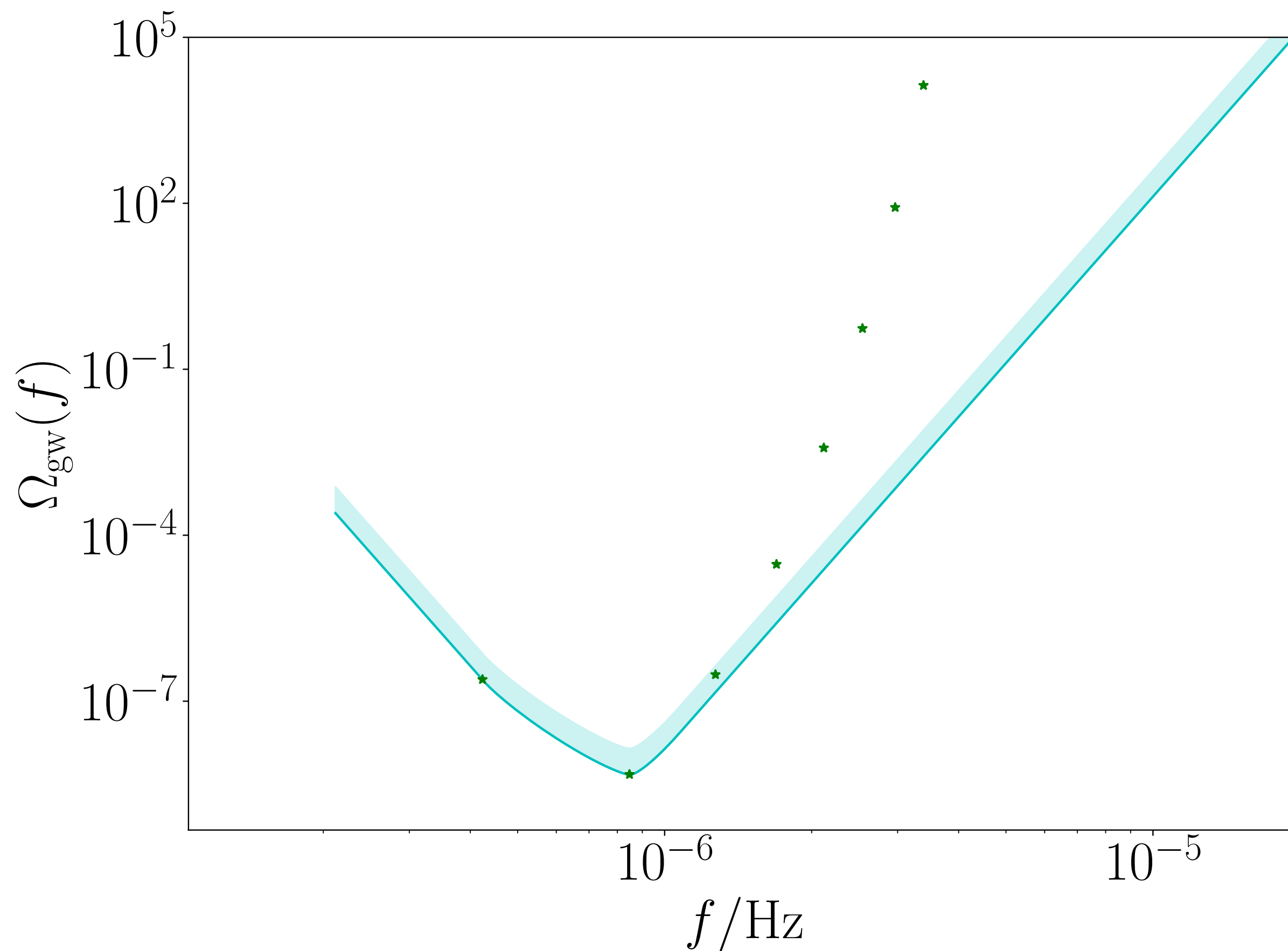
pulsar timing (J1638-4725), $e \approx 0.955$
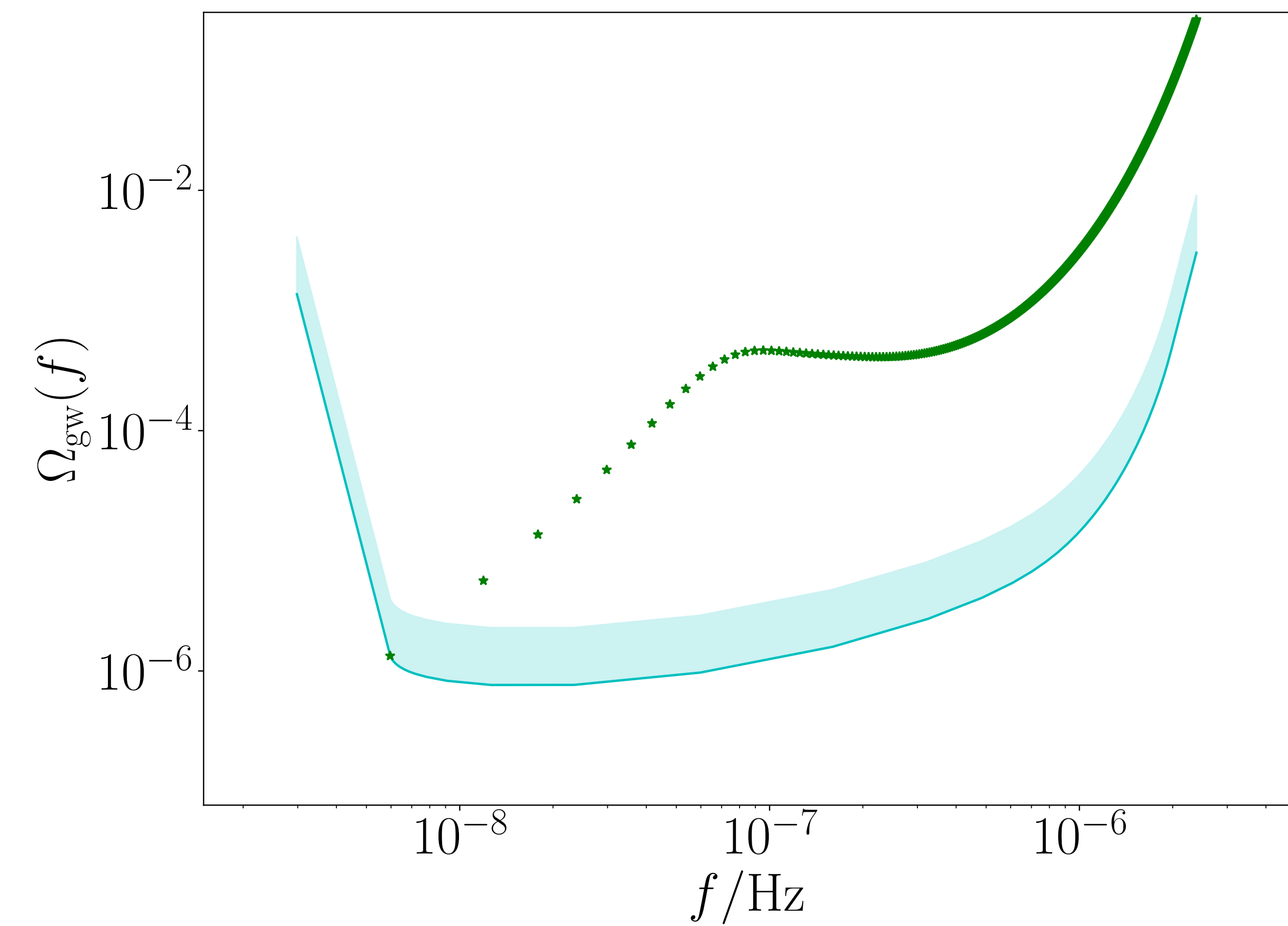
# Solar system bounds
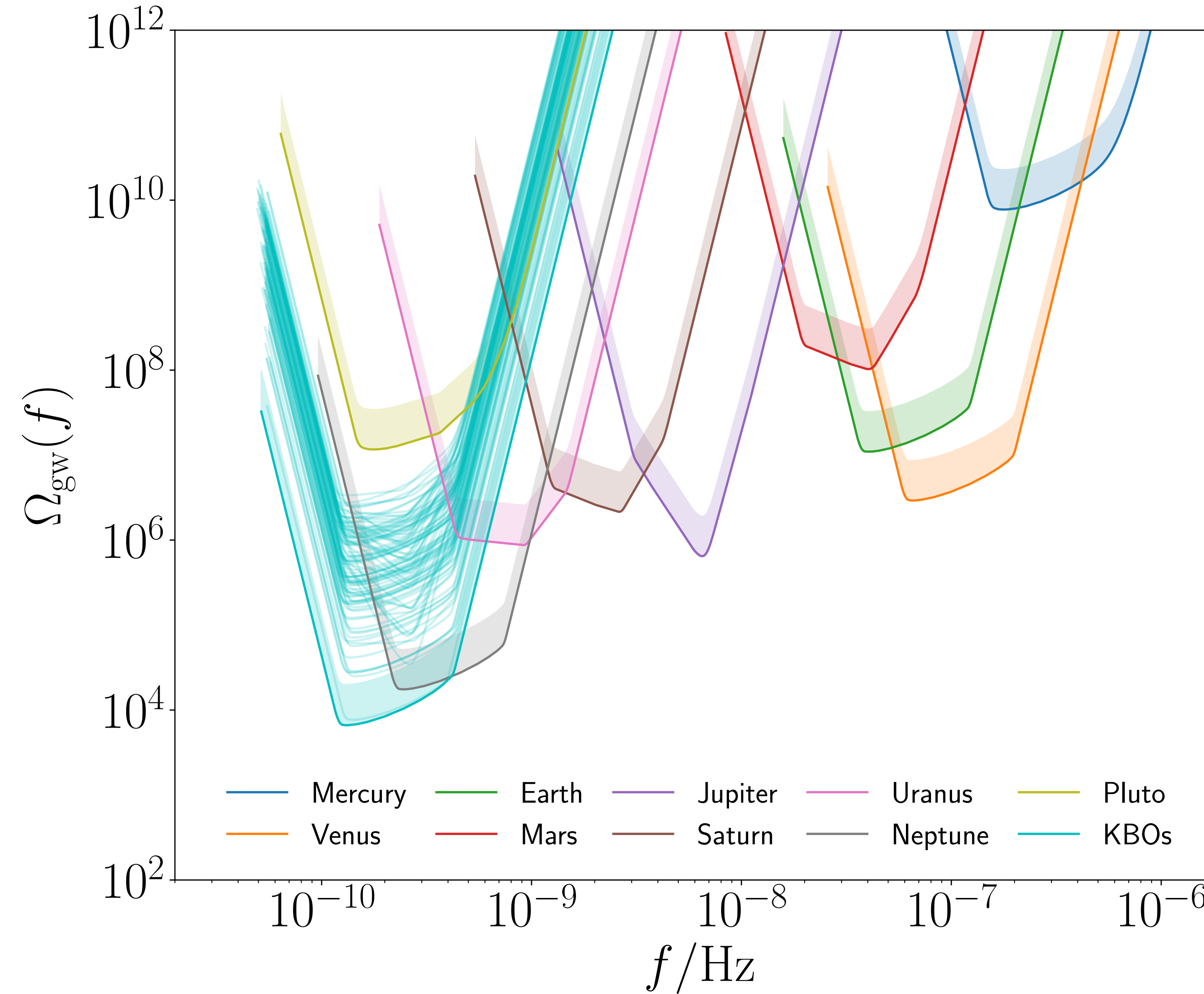
# Osculating orbits

$$\delta\ddot{\boldsymbol{r}} = r(\mathcal{F}_r\hat{\boldsymbol{r}} + \mathcal{F}_\theta\hat{\boldsymbol{\theta}} + \mathcal{F}_\ell\hat{\boldsymbol{\ell}}),$$

EoM is instead

$$\ddot{\boldsymbol{r}} + \frac{GM}{r^2}\hat{\boldsymbol{r}} = \delta\ddot{\boldsymbol{r}}.$$

$$\delta\ddot{r}^i = -\delta R^i{}_{0j0}r^j$$

$$\dot{P} = \frac{3P^2\gamma}{2\pi}\left[\frac{e\sin\psi\mathcal{F}_r}{1+e\cos\psi} + \mathcal{F}_\theta\right],$$

$$\dot{e} = \frac{\dot{P}\gamma^2}{3Pe} - \frac{P\gamma^5\mathcal{F}_\theta}{2\pi e(1+e\cos\psi)^2},$$

$$\dot{I} = \frac{P\gamma^3\cos\theta\mathcal{F}_\ell}{2\pi(1+e\cos\psi)^2},$$

$$\dot{\Omega} = \frac{\tan\theta}{\sin I}\dot{I},$$

$$\dot{\omega} = \frac{P\gamma^3}{2\pi e}\left[\frac{(2+e\cos\psi)\sin\psi\mathcal{F}_\theta}{(1+e\cos\psi)^2} - \frac{\cos\psi\mathcal{F}_r}{1+e\cos\psi}\right] - \cos I\dot{\Omega},$$

$$\dot{\varepsilon} = -\frac{P\gamma^4\mathcal{F}_r}{\pi(1+e\cos\psi)^2} - \gamma(\cos I\dot{\Omega} + \dot{\omega}),$$

$$(2.10)$$

# From Langevin to FP

$$\dot{X}_i(\boldsymbol{X}, t) = V_i(\boldsymbol{X}) + \Gamma_i(\boldsymbol{X}, t),$$

$$\frac{\partial W}{\partial t} = -\partial_i(D_i^{(1)}W) + \partial_i\partial_j(D_{ij}^{(2)}W),$$

with $\partial_i \equiv \partial/\partial X_i$.

$$D_i^{(1)} = V_i + \lim_{\tau \to 0} \frac{1}{\tau} \int_t^{t+\tau} \mathrm{d}t' \int_t^{t'} \mathrm{d}t'' \, \langle \Gamma_j(\boldsymbol{x}, t'')\partial_j\Gamma_i(\boldsymbol{x}, t') \rangle.$$

$$D_{ij}^{(2)} = \lim_{\tau \to 0} \frac{1}{2\tau} \int_t^{t+\tau} \mathrm{d}t' \int_t^{t+\tau} \mathrm{d}t'' \, \langle \Gamma_i(\boldsymbol{x}, t')\Gamma_j(\boldsymbol{x}, t'') \rangle.$$

# Examples of coefficients

$$D_P^{(1)} = V_P + \frac{9P^2\gamma^2}{4} \sum_{n=1}^{\infty} nH_0^2\Omega_n \left[ \left| E_n^{02} + \frac{e}{2}\left(E_n^{11} - E_n^{13}\right) \right|^2 - \frac{1+4e^2}{15}\left(S_n^{11}\right)^2 - \frac{e\gamma^2}{15}S_n^{11'}S_n^{11} \right.$$

$$+ \frac{\gamma^2}{10e}\left(E_n^{02} + \frac{e}{2}\left(E_n^{11} - E_n^{13}\right)\right)\left(3E_n^{11} + E_n^{13} + eE_n^{20} + 4E_n^{21} + 4eE_n^{22} - 4E_n^{23} - eE_n^{24} + 2E_n^{02'} + e\left(E_n^{11'} - E_n^{13'}\right)\right)^*$$

$$\left. - \frac{\gamma^4}{10e}E_n^{22}\left(E_n^{11} - E_n^{13} + 2E_n^{02'} + e\left(E_n^{11'} - E_n^{13'}\right)\right)^* \right]$$

$$D_{PP}^{(2)} = \frac{27P^3\gamma^2}{20} \sum_{n=1}^{\infty} nH_0^2\Omega_n \left[ \left| E_n^{02} + \frac{e}{2}\left(E_n^{11} - E_n^{13}\right) \right|^2 - \frac{\left(eS_n^{11}\right)^2}{3} \right]$$

# Covariance matrix over time

Schmitz, K. 2021
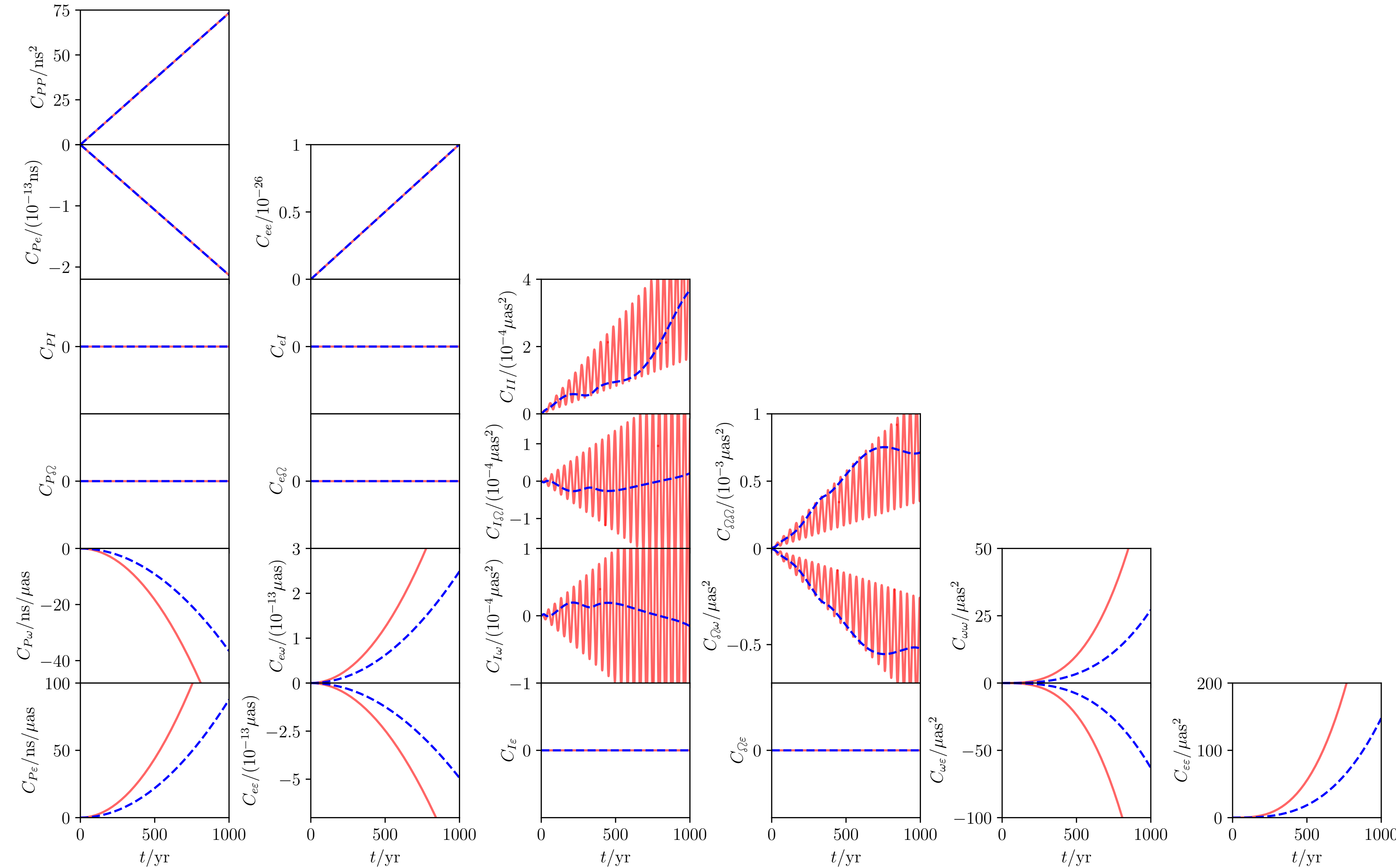
- four parameters:
  - ▶ temperature $T_*$
  - ▶ strength $\alpha$
  - ▶ rate $\beta/H_*$
  - ▶ bubble-wall velocity $v_w$

$$\Omega_{\mathrm{gw}}(f) = \Omega_{\mathrm{gw}}(f_*) \times (f/f_*)^3 \left[ \frac{7}{4 + 3(f/f_*)^2} \right]^{7/2}, \quad (14)$$

$$f_* \approx 19\,\mu\mathrm{Hz} \times \frac{T_*}{100\,\mathrm{GeV}} \frac{\beta/H_*}{v_w} \left( \frac{g_*}{106.75} \right)^{1/6}, \quad (5)$$

$$\Omega_{\mathrm{gw}}(f_*) \approx 5.7 \times 10^{-6} \times \frac{v_w}{\beta/H_*} \left( \frac{\kappa\alpha}{1+\alpha} \right)^2 \left( \frac{g_*}{106.75} \right)^{-1/3}$$
$$\times \left[ 1 - (1 + 2\tau_{\mathrm{sw}}H_*)^{-1/2} \right]. \quad (6)$$

speed of sound in the plasma). For the efficiency parameter $\kappa$ which appears in equation (6), we use the fitting functions in the appendix of Espinosa et al (2010),[85] while for the sound wave lifetime we take[86]

$$\tau_{\mathrm{sw}} = R_* \times \left( \frac{3\kappa}{4} \frac{\alpha}{1+\alpha} \right)^{-1/2}. \quad (16)$$